Understanding cognitive heterogeneity in Parkinson's disease:

Gerrits, N.J.H.M.

2015

document version
Publisher's PDF, also known as Version of record

Chapter 5

Reduced neural connectivity but increased task-related activity during working memory in *de novo* Parkinson patients

Authors
James P. Trujillo*
Niels J.H.M. Gerrits*
Dick J. Veltman
Henk W. Berendse
Ysbrand D. van der Werf#
Odile A. van den Heuvel#

*, # Both authors contributed equally to this work

Human Brain Mapping, 2015, 36(4), 1554-1566

ABSTRACT

Patients with Parkinson's disease (PD) often suffer from impairments in executive functions, such as working memory deficits. It is widely held that dopamine depletion in the striatum contributes to these impairments through decreased activity and connectivity between task-related brain networks, such as the fronto-parietal and fronto-striatal networks. We investigated this hypothesis by studying task-related network activity and connectivity within a sample of unmedicated patients with PD, versus healthy controls, during a visuospatial working memory task.

Sixteen *de novo* PD patients and 35 matched healthy controls performed a visuospatial *n*-back task while we measured their behavioural performance and neural activity using functional magnetic resonance imaging. We subsequently constructed regions-of-interest in the bilateral inferior parietal cortex (IPC), bilateral dorsolateral prefrontal cortex (DLPFC), and bilateral caudate nucleus to investigate group differences in task-related activity. We studied network connectivity by assessing the functional connectivity of the bilateral DLPFC and by assessing effective connectivity within the fronto-parietal and the fronto-striatal networks.

PD patients, compared with controls, showed trend-significantly decreased task accuracy, significantly increased task-related neural activity in the left DLPFC and a trend-significant increase in activity of the right DLPFC, left caudate nucleus and left IPC. Furthermore, we found reduced functional connectivity of the DLPFC with other task-related regions, such as the inferior and superior frontal gyri, in the PD group, and group differences in effective connectivity within the fronto-parietal network.

These findings suggest that working memory-related brain areas in PD patients show compensatory hyperactivation in order to maintain behavioural performance in the presence of network deficits.

INTRODUCTION

Patients with Parkinson's disease (PD) often suffer from non-motor symptoms, including cognitive deficits, especially in the so-called executive functions [157-160]. The loss of dopamine producing neurons of the substantia nigra pars compacta and ventral tegmental area [161, 162] results in a hypo-excitation of the fronto-striatal networks that presumably underlie the executive dysfunctions, such as working memory impairment [32, 33].

Working memory refers to the process of temporarily storing and manipulating information in the face of on-going processing for use in goal-directed behaviour [163, 164]. An often-employed task to assess working memory capabilities is the *n*-back paradigm: a well-established task due to its reliability and the ease of manipulating processing load [165]. Neuroimaging studies have consistently shown that task performance on the *n*-back paradigm is associated with activity of the fronto-striatal network (i.e. bilateral dorsolateral prefrontal cortex (DLPFC) and bilateral caudate nucleus) and fronto-parietal network (i.e. bilateral inferior parietal cortex (IPC) and bilateral DLPFC [26, 166-169].

Adequate dopaminergic neurotransmission in the striatum also plays an important role in task performance on working memory tasks [170, 171]. A recent study by Ekman and colleagues [172] reported decreased *n*-back performance in patients with PD diagnosed with mild cognitive impairment (MCI), compared with PD patients without MCI, associated with reduced levels of dopamine-transporter binding in the right caudate nucleus, as measured by single photon emission tomography (SPECT).

Cools and D'Esposito [173, 174] argue that optimal dopamine levels lead to a stable working memory representation by "quelling" the activity of all but the most active cells and increasing the excitability of inhibitory neurons. This results in an increased signal-to-noise ratio between neuronal populations and thus in better communication. Also functional brain imaging shows that optimal dopamine levels lead to more focused activity, whereas depletion leads to increased and more widespread [175] activation which correlates positively with task errors [176], supporting the notion of dopaminergic modulation of functional brain networks. Lower dopamine receptor stimulation in patients with PD would thus lead to an impairment in working memory updating (i.e. replacing old / irrelevant information with new / relevant information online in the working memory), and consequently a decreased working memory performance. Brittain and Brown [177] argue in a similar fashion that dopamine depletion in PD results in decreased synchronization between neural populations in frequencies associated with information exchange, with an increase in inhibitory frequency bands. They state that dopaminergic medi-

cation normalizes this pathological synchronization and that the degree of normalization positively correlates with improvements in clinical motor scores.

These findings suggest that dopamine plays an important role in the synchronization and connectivity between brain areas. By investigating both task-related functional connectivity as well as neural activity in *de novo* PD patients, we can obtain an unbiased view on how PD-related neural changes relate to behavioural task performance in early PD. Methodologically, studying *de novo* patients is important because dopaminergic medication down-regulates dopamine receptor density in the striatum [178], therefore the observed effects of PD in relation to dopamine on, for example, task-related networks may influenced by medication use.

In order to gain more insight into the relation between working memory capacity and task-related network connectivity in patients with PD, we measured behavioural performance and task-related neural activation in de novo PD patients during a visuospatial *n*-back task. Analyses focused on the bilateral IPC, DLPFC, and caudate nucleus, representing the most crucial areas within the fronto-parietal and fronto-striatal networks. In addition to the general linear model (GLM) analyses of activation, we assessed the task-related functional connectivity of the bilateral DLPFC using psycho-physiological interaction [PPI 179] analyses and the effective connectivity between our regions-of-interest (ROIs) using dynamic causal modelling (DCM) [180]. We hypothesized that PD patients, compared with controls, would show decreased task accuracy, accompanied by decreased task-related neural activation, reduced task-related functional connectivity of the DLPFC with other task-related areas, and altered effective connectivity within the fronto-parietal and fronto-striatal networks.

MATERIALS AND METHODS

Participants

Twenty-five non-demented, de-novo patients with PD and 40 healthy controls participated in this study. A number of participants was excluded before MR imaging due to an inability to perform the task (6 patients; 3 controls); these participants had difficulty understanding or carrying out the task correctly, even during training sessions. Initial analysis led to the exclusion of several additional participants due to poor quality of the functional MRI images (2 patients), and extreme scores on inaccuracy (more than two standard deviations from the median) in comparison with their own group (1 patient; 2 controls), rendering our total sample size 16 patients with PD (mean age: 58.3 years ± 9.5) and 35 healthy controls (mean age: 55.5 ± 9.5) (see table I for demographic data). Education scores repre-

sent the highest level of completed education based on the division by Verhage [181]. Patients were diagnosed by a movement disorder specialist according to the UK PD Brain Bank criteria [100] for idiopathic PD in addition to abnormal dopamine transporter single-photon emission computed tomography (DaT-SPECT) scans where available. Patients had not yet begun dopaminergic or cholinergic medication at the time of the investigation. The Unified PD Rating Scale Part III (UPDRS-III) [101] and Hoehn and Yahr stage [102] were administered to assess disease severity and stage, respectively. We determined disease subtype (i.e. tremor dominant / akinetic) and disease lateralisation based on the scores using the method described by Eggers and colleagues [182]. All participants were screened for general cognitive status using the Mini-Mental State Examination (MMSE) [104], depressive symptoms using the Beck Depression Inventory [BDI 183] and anxiety using the Beck Anxiety Inventory (BAI) [106]. We screened for the presence of psychiatric disorders using the Structured Clinical Interview for DSM-IV Axis-I Disorders (SCID-I) [103]. None of the participants had a score of <24 on the MMSE, or >15 on the BDI. Handedness was assessed using the Edinburgh handedness inventory [107]. All participants provided informed consent, obtained according to the Declaration of Helsinki, and the study protocol was reviewed and approved by the Medical Ethical Committee of the VU University Medical Center.

Working memory paradigm:

We assessed working memory using a visuospatial version of the *n*-back task (for details, see De Vries et al, 2013 [184]). In short, participants were visually presented with a grey diamond figure in which four large blue dots were positioned, which were randomly replaced by a yellow dot. Working memory load was increased consecutively by asking the participants to respond, using the index finger of their dominant hand, to the location of the present dot (N0), previous dot (N1), or with a delay of two (N2) or three stimuli (N3) via an MRI compatible response box. Participants were familiarized with the task in a practice session prior to the experiment.

Image acquisition

Functional MRI data were acquired on a GE Signa HDxt 3-T MRI scanner (General Electric, Milwaukee) at the VU University Medical Center using a gradient echo-planar imaging (EPI) sequence (TR = 2100 ms; TE = 30 ms; 64 x 64 matrix; field of view = 24 cm; flip angle = 80°) with 40 ascending slices per volume (3.75 x 3.75 mm in-plane resolution; slice thickness = 2.8 mm; inter-slice gap = 0.2 mm), which provided whole-brain coverage. Structural scanning included a sagittal three-dimensional gradient-echo T1-weighted sequence (256 x 256 matrix; voxel size = 1 x 0.977 x 0.977 mm; 172 sections).

Data Analysis

Behavioural data

We assessed working memory performance by calculating the overall percentage of correct responses within each condition per participant. We compared the two groups using a mixed ANOVA with task-load (levels: N0 / N1 / N2 / N3) as within-subject factor and group (levels: patients with PD / healthy controls) as between-subject factor, while employing the Greenhouse-Geisser correction when the assumption of sphericity was violated.

Image processing and analysis

Pre-processing and statistical analyses were performed in SPM8 (Wellcome Department of Imaging Neuroscience, London, UK) running in Matlab (version 7.5, The MathWorks Inc., Natick, MA, 2000). The EPI images were first slice-time corrected, then realigned to the first image and unwarped using a least squares approach and a six parameter (rigid body) spatial transformation to correct for motion. They were subsequently warped to the Montreal Neurological Institute (MNI) T1-template, employing the individual T1-weighted image for estimation. Lastly, the images were smoothed with an 8 mm Gaussian kernel.

A design matrix was created in order to examine within-subject effects in a first level GLM. We employed a block design modelling all trials within each of the four conditions with a fixed duration of 56 seconds. The first regressor was labelled "N0", the second "N1", the third "N2", and the fourth "N3", and the six movement parameters that were calculated during the realignment were added to the model as covariates of non-interest. The contrast of interest, the "task-effect" contrast, was defined as "N3N2N1>N0", which was used for the whole brain GLM, region of interest, gPPI and DCM analyses to examine the effect of working memory, corrected for baseline features of the task such as visuospatial processing and motor responses.

Contrast images derived from the first level analyses were used at the second (group) level, employing whole-brain voxel-wise independent t-tests. Brain regions were identified using the WFU-Pick Atlas [151]. Whole-brain statistical maps were thresholded at $p < .05$ corrected for family-wise errors (FWE) in the main effects. Whole-brain results represent a pooled analysis of both controls and patients together (n=51) and are subsequently used as described in the proceeding sections.

Whole-brain assessment of the effect of load (N3>N2>N1>N0) showed that these results were comparable to the 'task-effect' contrast, and for purposes of comprehensibility we do not discuss these results here. All subsequent analyses are based on the task-effect contrast.

Regions of interest

We defined ROIs around the peak-voxel coordinates of the main effect of working memory (i.e. N1N2N3>N0) over all subjects (N=51; see Supplementary Table 5.1), using MarsBaR (http://marsbar.sourceforge.net). Spherical ROIs with a 5 mm sphere were constructed for the left and right DLPFC (BAs 9/46; right: x= 39, y= 32, z= 31; left: x= -42, y= 26, z= 31) and with a 10mm sphere for the IPC (BA 40; right: x= 51, y= -52, z= 40; left: x= -48, y= -49, z= 46). These coordinates were used as initial starting points, after which the center of the sphere was automatically moved to the nearest local maximum using SPM8's volume of interest (VOI) utility in each participant to account for the individual variability between participants and to increase sensitivity. Each peak was manually checked to ensure it was still in the designated region.

The average parameter estimates of the whole ROI were then extracted from the task-effect contrast per participant and were subsequently compared using 2-sample t-tests in SPSS 20 (SPSS, Chicago, IL, USA). For these analyses we calculated a Bonferroni-adjusted alpha value using Simple Interactive Statistical Analysis (http://www.quantitativeskills.com/sisa/calculations/bonfer.htm) that took into account the mean correlation coefficient between all ROIs to correct for multiple comparisons. The mean correlation coefficient between all six ROIs was r = .48, leading to a Bonferroni adjusted alpha value of p = .02.

Time-courses were extracted from each of the individual ROIs, using the task-effects contrast, creating VOIs for use in the connectivity analyses. These were extracted at a 0.1 threshold in order to ensure robust time-series.

Functional connectivity: gPPI

We assessed the task-related functional connectivity of the left and right DLPFC using a generalized form of context-dependent psychophysiological interaction (gPPI [179, 185]). A PPI analysis statistically tests in a whole-brain voxel-wise manner whether areas outside the seed region are functionally connected to the seed region during the task [179]. We chose gPPI, instead of the traditional PPI [186], as it allowed us to model all psychological task conditions into one first-level design, thus improving the model-fit [185]. We used the individually determined left and right DLPFC ROIs from the GLM analysis as seed regions.

Our first-level model included the four task conditions, the four convoluted PPI terms, the time-series of the seed-region, and the six movement parameters. We again defined the contrast "N1N2N3>N0", this time using the convoluted PPI terms and leaving the psychological variable (task conditions) and movement parameters as covariates of no interest. Subjects were excluded from this analysis if no BOLD time-course could be extracted due to a lack of active voxels within the region of interest, or if there were no voxels that were functionally connected to the seed region. After exclusion, 15 patients and 32 controls were included in the analysis of the left DLPFC, and 14 patients and 33 controls were included for the right DLPFC.

At the second level, we compared the contrast N1N2N3>N0 between groups using an independent samples t-test and an uncorrected statistical threshold of $p < .001$ with a spatial extent threshold of $k > 5$, while masking inclusively for the main effect of task. The same analysis procedures were employed for the left and right DLPFC.

Effective connectivity: DCM

In order to gain more insight into the connectivity within the fronto-parietal (i.e. left and right DLPFC and left and right IPC) and the fronto-striatal (i.e. left and right DLPFC and caudate nucleus) network, we calculated the effective connectivity using deterministic DCM [180]. In short, DCM constructs several forward-models that predict how the BOLD signal would behave if certain connections between the interacting regions are present. It tests if the signal is driven or modulated at a certain connection or specific region. After computing all models and connections, an algorithm statistically tests which model best fits the observed data.

For the fronto-striatal network, the intrinsic connections between the left and right DLPFC were modelled in a bidirectional way, with efferent connections from each DLPFC to the ipsilateral caudate nucleus based on literature [187, 188]. By varying the driving and modulatory effects of working memory within the fronto-striatal network, a total of 7 models was created (see Supplementary Fig. 5.1). For this analysis, the individually determined DLPFC VOIs, described above, were used together with time-courses extracted from masks defining the whole left and right caudate nucleus, as found in the automated anatomical labelling (AAL) software package. After exclusion, the analysis included 13 patients and 34 controls.

For the fronto-parietal network, intrinsic connections were again assumed to be bidirectional between left and right DLPFC, with bidirectional connections be-

tween the DLPFC and ipsilateral IPC as well as between left and right IPC. Because anatomical and functional connectivity were less clearly defined for this model-set, we generated four families of models. The families modelled top-down, bottom-up and mixed processing, with the final family consisting of one model that utilized all possible inputs. This resulted in a total of 24 fronto-parietal models (see Supplementary Fig. 5.2). This analysis used the individually created VOIs for the bilateral DLPFC and IPC. After exclusion, 15 patients and 24 controls were included in this analysis.

We used Bayesian Model Selection (BMS) to statistically test the probability of the observed data given the model. To account for the heterogeneity of network dynamics resulting from neurodegeneration we employed a random effects (RFX) approach, rather than the standard fixed effects approach [189]. Once the model-evidences have been computed for the models in each subject, the exceedance probability (Φ) can be calculated for the model-set. This is the probability that a model is more likely than any other to have generated the observed BOLD signal.

Correlation with dopamine transporter binding

For 12 out of the 16 PD patients, SPECT scans with a [^{123}I]FP-CIT tracer binding to the DaT were available with an average interval between SPECT acquisition and MRI acquisition of 55 (range: 26 – 123) days. We used these scans to calculate the age-corrected binding ratios (ratio of specific to non-specific DaT binding, with the occipital lobe as a reference for non-specific binding) in the dorsal-medial striatum (procedure and calculation described elsewhere [190]) in order to perform a post-hoc analysis on the relation between striatal dopamine levels and task performance (using a correlation analysis on [^{123}I]FP-CIT uptake ratios and overall task accuracy) and task-related network connectivity. We entered the [^{123}I]FP-CIT uptake ratios as covariates into a 2nd level whole-brain regression analysis of our gPPI data for both the left and right DLPFC. Since this entailed an exploratory analysis, the results were considered significant at a threshold of $p < .001$ (uncorrected), with no spatial extent threshold.

RESULTS

The groups were matched with respect to age, gender, education, and handedness (see Table I) and did not differ on MMSE scores ($U = 336$, $p = .22$). PD patients, compared with healthy controls, had higher MADRS ($U = 143$, $p = .004$), BDI ($U = 175$, $p = .04$) and BAI scores ($U = 114$, $p = .001$), but these scores were far below accepted thresholds for mild depression or anxiety and therefore not clinically

relevant. The mean UPDRS and median Hoehn and Yahr stage of the PD patients were 22 and two, respectively.

Behavioural results

We found that patients with PD, compared with controls, had trend-significantly lower overall accuracy scores ($F(1,49) = 3.54$; $p = .06$, see Fig. 5.1). The accuracy scores significantly decreased with increasing task-load ($F(2.09,102.2) = 104.53$; $p < .001$), and this effect did not differ between patients and controls ($F(2.09,102.2) = 1.66$; $p = .19$).

Table 5.1 Demographic, clinical, and behavioural characteristics Values are presented as mean ± standard deviation or median (range) unless indicated otherwise.

	PD patients (n=16)	Controls (n=35)	*p*-value
Demographics			
Age	58 ± 10 (38 – 74)	56 ± 9 (38 - 70)	0.34
Sex (% male)	11 (69%)	20(57%)	0.44
Handedness (% right)	14 (88%)	31 (89%)	0.55
IQ	105 ± 19 (82 – 142)	104 ± 15 (73 – 132)	0.85
Education	5.87± 0.9 (4 – 7)	5.69± 1.1 (3 – 7)	0.54
Clinical measures			
MMSE	28.81± 0.8 (28 – 30)	29.11± 0.8 (3 – 27)	0.22
MADRS	1.88± 2 (0 – 4)	0.82 ± 2 (0 – 7)	0.004
BAI	4.63 ± 3 (0 – 9)	1.6 ± 3 (0 – 10)	0.001
BDI	4.00 ± 4 (0 - 11)	2.20 ± 3 (0 - 11)	0.04
UPDRS-III	21.63 ± 9 (2 – 35)		
Subtype (% tremor / % akinetic)	1 (7%) / 10 (67%)		
Lateralization (% left / % right)	6 (40%) / 2 (13%)		
Hoehn & Yahr	2 (1 – 3)		
Disease duration	2.69 ± (0 – 7)		
Behavioural measures			
Total *n*-back accuracy	74 ± 14 (47 – 90)	82 ± 13 (58 – 100)	0.06
n-back (*n* = 0)	95.13 ± 12 (52 – 100)	98.97 ± 5 (70-100)	0.23
n-back (*n* = 1)	90.63 ± 13 (52 – 100)	93.62 ± 11 (53 – 100)	0.39
n-back (*n* = 2)	64.69 ± 24 (23 – 98)	76.52 ± 22 (28 – 100)	0.09
n-back (*n* = 3)	46.35 ± 20 (15 – 78)	59.48 ± 24 (22 – 100)	0.08

MMSE: Minimal Mental State Examination; MADRS: Montgomery-Åsberg Depression Rating Scale; UPDRS: Unified Parkinson's Disease Rating Scale; BAI: Beck Anxiety Inventory; BDI: Beck Depression Inventory.

Imaging results

Main effect of task

The whole-brain main effect of task (contrast: N1N2N3>N0) showed significant activation of the bilateral IPC, bilateral DLPFC, bilateral ventrolateral prefrontal cortex (VLPFC), left middle frontal gyrus, left precuneus, left medial frontal gyrus, right middle temporal gyrus, bilateral posterior cingulate cortex, left superior temporal gyrus, the right cuneus, right caudate nucleus (see Supplementary Table I). For the effect of task per group, see Supplementary Table II; for group x task comparisons, see Supplementary Table III.

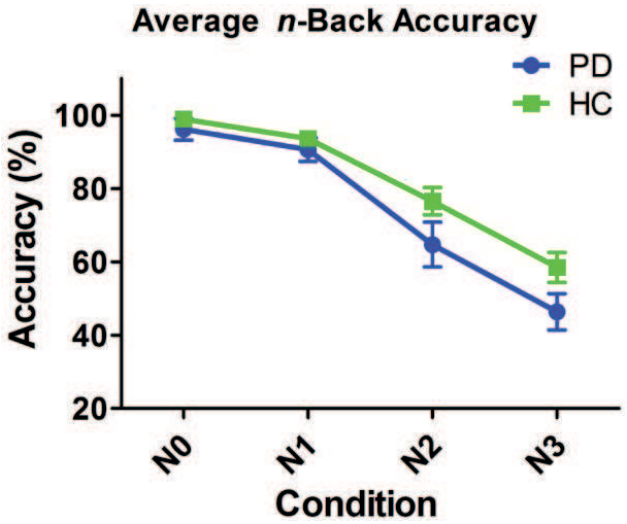

Figure 5.1. Average n-Back accuracy Mean accuracy scores (represented on the *y*-axis), in percentages, for each group across the four conditions (displayed on the *x*-axis); The blue line represents the PD group, and green line represents the healthy controls, while the error bars display the standard error of the mean. Overall a trend toward lower accuracy (p = .06) was found in the Parkinson's group.

ROI Analyses

PD patients, compared with healthy controls, showed a significant increase in task-related activation in the left DLPFC (t (21.36) = 2.65, p = .01, see Fig. 5.2) and a trend-significant increase in the right DLPFC (t (49) = 2.25, p = .03). The PD patients also showed a trend-significant increase in the left caudate nucleus (t (49) = 1.8, p = .08) but not in the right caudate nucleus (t (49) = 1.48, p = .15), as well as a trend-significant increase in the left IPC (t (49) = 2.28, p = .03), but not in the right IPC (t (49) = .99, p = .33) when compared with controls.

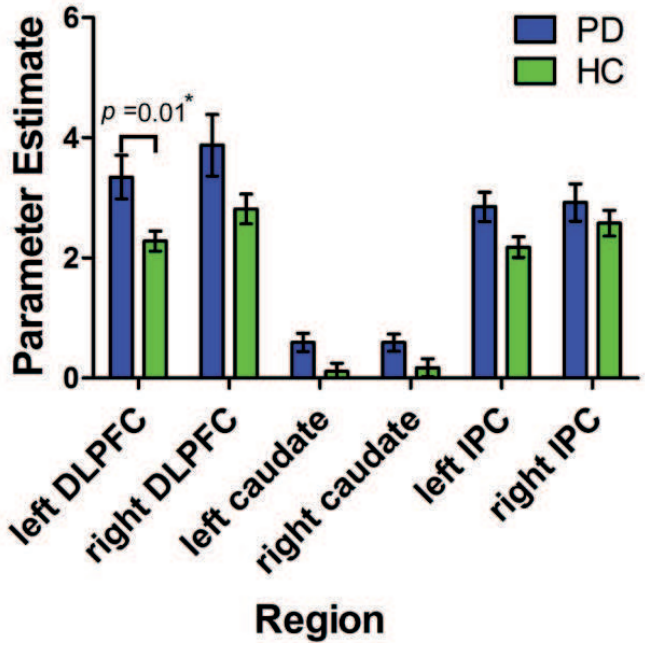

Figure 5.2. Average n-Back accuracy Mean parameter estimates extracted from the task-effect contrast (N3N2N1>N0) per ROI per group. Blue bars represent the PD group, while the green bars represent the healthy controls. The y-axis indicates the mean parameter estimates, and the x-axis depicts the six ROIs. P-values are given for the ROIs that differed in activation between the groups. * significant after correction for multiple comparisons. Error bars represent the standard error of the mean. DLPFC, dorsolateral prefrontal cortex; IPC, inferior parietal cortex; HC, healthy controls; PD, patients with PD; ROI, region of interest.

gPPI

Compared to the PD patients, the control group showed stronger positive coupling between the left DLPFC and the bilateral middle frontal gyrus, bilateral precuneus, left insula, and the right superior frontal gyrus; no areas of stronger negative coupling were found in the controls compared with the PD patients. Patients showed no regions of stronger positive coupling compared with controls, but did show stronger negative coupling between the left DLPFC and the bilateral superior frontal gyrus, bilateral precuneus, left insula and left inferior frontal gyrus. Table 5.2 provides a full overview of these group comparisons and Fig. 5.3 provides a graphic representation of how groups typically differed in coupling direction for the same regions. For the main effects of the left DLPFC within each group (see Supplementary Table 5.4).

The control group, compared with PD patients, showed stronger positive coupling between the right DLPFC and the left VLPFC and left superior frontal gyrus, but

no stronger negative coupling. When comparing the patients with the controls, we found stronger negative coupling between the right DLPFC and the bilateral VLPFC, left superior frontal gyrus and left cerebellum, but no stronger positive coupling. Table 5.3 provides an overview of these interaction effects. For the main effects of the right DLPFC within each group, see Supplementary Table 5.5.

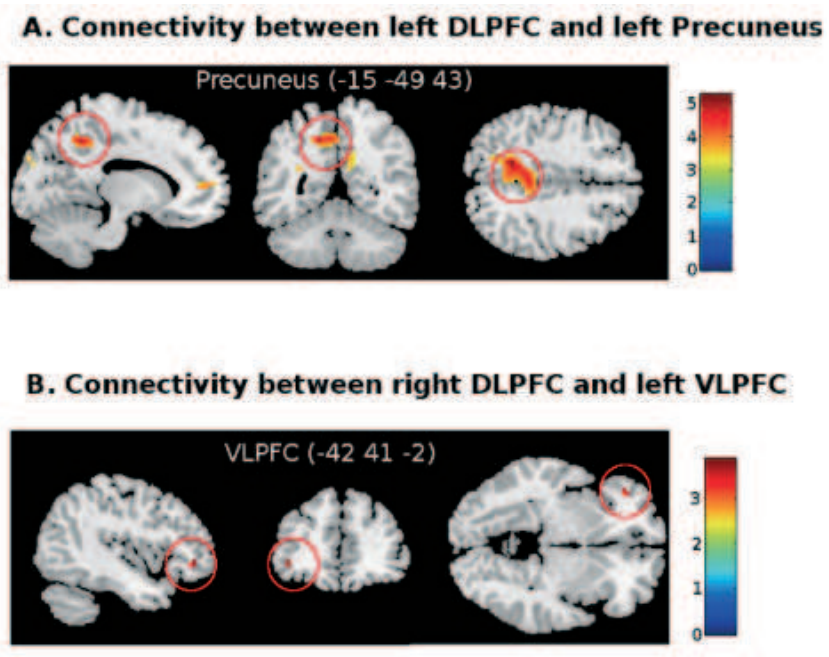

Figure 5.3 Functional connectivity maps showing opposite coupling in the controls and Parkinson's patients. On the left, the cluster corresponding to a representative cluster is indicated on a standardized T1 MR image, with the name of the representative region and the peak coordinates in MNI space. The colour gradient legend represents the *Z*-scores. On the right, the bar-graph represents strength of coupling between the seed region and the representative region. Group is represented on the *x*-axis and degree of coupling on the *y*-axis. Pink lines show the standard error of the mean. A. Connectivity between the left DLPFC and the left precuneus. B. Connectivity between the right DLPFC and the left VLPFC.
DLPFC, dorsolateral prefrontal cortex; HC, healthy controls; MNI, Montreal Neurological Institute; MR, magnetic resonance; PD, patients with PD; VLPFC, ventrolateral prefrontal cortex.

Table 5.2 Whole-brain analysis of group differences in gPPI effects for left DLPFC. Significant at a threshold of p = .001 (uncorrected) with an extent-threshold k>5.

		Controls > PD patients					PD patients > Controls				
BA	Area	T-value	Cluster size	Peak coordinates (MNI)			T-value	Cluster size	Peak coordinates (MNI)		
				X	Y	Z			X	Y	Z
				Positive Coupling							
10	Middle frontal gyrus	5.01	36	-24	56	13					
10		3.93	18	15	47	7					
31	Precuneus	4.91	126	-15	-49	43					
7		4.76		-6	-49	46					
7		4.58		3	-37	46					
31		3.55	16	9	-52	28					
13	Insula	4.06	67	-48	-43	16					
32	Anterior cingulate cortex	3.89	18	6	44	10					
9	Dorsolateral prefrontal cortex	3.89	15	-36	5	34					
8	Superior frontal gyrus	3.67	16	3	23	58					
19	Cuneus	3.62	7	-15	-91	28					
	Putamen	3.54	6	33	-7	-11					
				Negative Coupling							
10	Superior frontal gyrus						5.26	173	-21	56	10
8							3.67	13	3	23	58
7	Precuneus						4.91	191	-15	-49	43
7							4.58		3	-37	46
31							3.55	17	9	-52	28
13	Insula						4.06	141	-48	-43	16
							3.64	7	36	-13	-8
42	Superior temporal gyrus						3.69	9	-63	-28	10
39	Lateral occipirtal gyrus						3.79		-36	-73	13
18	Cuneus						4.02	37	-18	-79	19
9	Inferior frontal gyrus						3.89	5	-36	5	34
4	Precentral gyrus						3.82	11	48	-16	37
32	Anterior cingulate cortex						3.82	16	18	35	13

Table 5.3 Whole-brain analysis of group differences in gPPI effects for right DLPFC. Significant at a threshold of p = .001 (uncorrected) with an extent-threshold k>5.

		Controls > PD patients					PD patients > Controls				
BA	Area	T-value	Cluster size	Peak coordinates (MNI)			T-value	Cluster size	Peak coordinates (MNI)		
				X	Y	Z			X	Y	Z
				Positive Coupling							
47	Ventrolateral prefrontal cortex	3.73	5	-42	41	-2					
6	Superior frontal gyrus	3.34	5	-6	8	67					
				Negative Coupling							
	Cerebellum						3.89	14	0	-49	-11
47	Ventrolateral prefrontal cortex						3.73	5	-42	41	-2
47							3.62	10	33	23	-8
6	Superior frontal gyrus						3.34	5	-6	8	67

DCM

In the *fronto-striatal* analysis, although the exceedance probability of model two (PD: Φ = 0.0001; Controls: Φ = 0.002) was significantly smaller than the other six models in both groups (PD: Φ-range = 0.15 to 0.18; Controls: Φ-range = 0.15 to 0.19), no best fit model could be determined amongst the remaining six models for the healthy controls or the PD group.

Model selection of the *fronto-parietal* set revealed, for the healthy controls, that model 4, i.e. direct driving of the left DLPFC with modulation of the ipsilateral DLPFC/IPC connection, was the best fit (Φ = 0.99). In the PD group on the other hand, model 19 (driving effect of left DLPFC and left IPC; Φ = .64) provided the best fit, although model 4 also had a high exceedance probability (Φ = 0.32). Fig. 5.4 shows the models with the best fit.

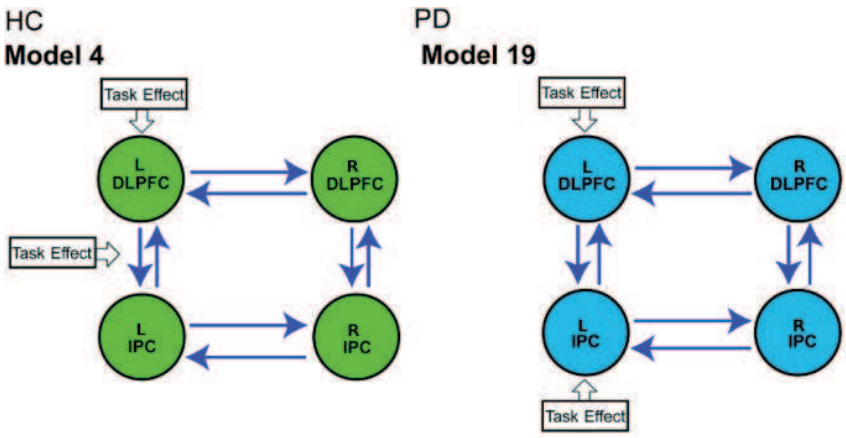

Figure 5.4 Best-fit models from the frontoparietal BMS set. Circles represent the regions included in the model-space, blue arrows represent intrinsic connections, open arrows with "task effect" label pointing toward a region represent driving effects, and open arrows with the "task effect" label pointing toward intrinsic connection represent modulation of these connections. On the left: model 4, representative of the control group; on the right: model 19, representative of the patient group.

Dopamine Transporter Binding

Assessment of dopamine transporter binding in the dorsomedial striatum revealed a positive correlation between binding ratios and task performance, r = .65, p = .02 (see Fig. 5.5).

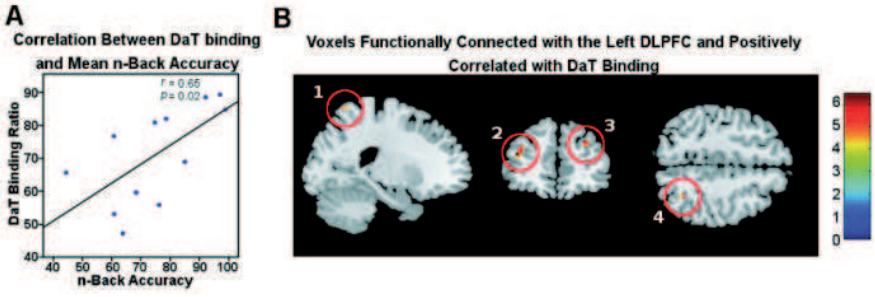

Figure 5.5 Significant positive correlations between dopamine-transporter binding ratios in the dorsomedial caudate nucleus and (A) task performance and (B) functional connectivity with the left DLPFC. In A, the *y*-axis displays dopamine-transporter binding ratios, while the *x*-axis represents accuracy scores, in percentage, on the *n*-back task; B shows voxels functionally connected to the left DLPFC, as described in the gPPI analysis, which correlated positively with dopamine-transporter binding ratios. From left to right the circled regions are the left postcentral gyrus (1), the bilateral middle frontal gyrus (2–3), and the right superior parietal lobe (4).

We also found that higher dopamine transporter binding levels in the dorsomedial striatum were associated with increased functional connectivity between the left DLPFC and the bilateral middle frontal gyrus (left: $t = 6.5$; right: $t = 6.2$), the right superior parietal lobe ($t = 5.2$), and the left postcentral gyrus ($t = 4.7$).

No voxels reached the statistical threshold when investigating the relation between dopamine transporter binding ratios and functional connectivity of the right DLPFC.

DISCUSSION

This study examined the fronto-striatal and fronto-parietal network in unmedicated patients with PD during the performance of a visuospatial working memory task. In sum, we found that patients compared with controls displayed a mild behavioural deficit, increased task-related recruitment of the left DLPFC (related to level of dopaminergic degeneration), decreased functional connectivity of the bilateral DLPFC with other brain regions within the networks, and altered fronto-parietal connectivity, with a more driving role for the IPC. These results suggest that the functional network integrity, and communication between different brain areas, is reduced in patients with PD. We hypothesize that the impaired connectivity between the task-related brain areas is caused by PD-related dopamine depletion and is compensated for by the hyperactivation of the individual task-related brain areas.

Behavioural performance in the PD patients was only marginally affected when compared with the control group. Although numerous studies reported significant impairments in working memory performance in PD patients, even in the early stages of the disease [191, 192], at least one other study on working memory in unmedicated patients with PD also found no significant decrease in task-performance [193]. Our patients had a relatively high education level (although matched with the control group) and we speculate that this might have served as a protective factor against cognitive decline [194], either by reduced cognitive decline or increased cognitive reserves, allowing our patient group to maintain reasonably good performance.

As expected, the analyses on the combined study population, involving both patients and controls, showed a robust effect of task in the bilateral inferior parietal and prefrontal areas: areas known to be involved in working memory [195]. The PD patients, compared with controls, showed significantly increased activation in the left DLPFC and a trend-wise increased activation in the right DLPFC, left

caudate nucleus, and left IPC. *Hyper*activation of task-related brain areas accompanied by (near) intact behavioural performance is a well-known phenomenon in both healthy aging [196] and disease [184, 197] and is often interpreted as a compensatory mechanism. In contrast, *hypo*activation is associated with decreased task-performance [172, 198], and we hypothesize that when the compensatory hyperactivation no longer suffices, the task-related brain areas will convert from hyper- to hypoactivation and the behavioural performance will decrease accordingly.

We found that the left and right DLPFC of healthy controls, compared with PD patients, was functionally more strongly connected with prefrontal regions, the precuneus, and insula during task performance. The disease-related changes, such as the striatal dopamine depletion, likely mediate reduced functional connectivity, underscoring the important role of dopamine in orchestrating connectivity between areas during task performance. Previous studies have shown that dopamine plays an important role in enhancing the signal-to-noise ratio between assemblies of neurons [199], and that it plays an important part in the connectivity between different brain areas [200]. Negative coupling exists between task-related networks and the default mode network and indicates a suppression of the default mode network by the task-related network [201]. Our finding of increased negative coupling therefore, with little to no positive coupling, within and between task-related functional networks in unmedicated PD patients provides further evidence that a decline in striatal dopamine results in highly impaired information exchange, possibly leading to inhibition within the task-related network. This pattern of connectivity reversal in PD patients compared to controls was also reported by Wu and colleagues [202]. This hypothesis is further strengthened by our positive correlation between pre-synaptic striatal dopamine levels and connectivity between the left DLPFC and other (prefrontal) areas.

Our group and others have found increased connectivity during rest [203-205], which seems to support the hypothesis that the inability to adequately suppress resting state networks results in the inability to switch to task-specific functional networks. A second possible explanation for the opposing direction of altered network connectivity at rest and during task performance relates to the difference in methodology of the aforementioned studies compared to the current study. The mentioned resting state results were based on electroencephalogram (EEG) and magnetoencephalogram (MEG) data and concerned global connectivity in the form of oscillatory synchronization in various frequency bands. Therefore, while global connectivity is increased, connectivity within task-specific networks may be decreased. This explanation is largely in line with the theory of decreased signal-to-noise ratio as overall connectivity increases while functional efficiency decreases.

Since executive functioning relies on the activation of the prefrontal cortex and its ability to functionally connect with other frontal and posterior regions [206], our results provide an explanatory model as to why PD patients have difficulties with working memory tasks. Although largely in agreement with our findings and hypotheses, we suggest some caution in directly comparing our study with those discussed above, as our study focused on task-related systems as measured by fMRI, while those of Olde Dubbelink [73], Silberstein [207], and Stoffers [76] measure the brain at rest using MEG/EEG.

The effective connectivity analyses in the healthy controls showed a best-fit with a top-down model of processing in the fronto-parietal network, with the DLPFC as the main driving region and task-modulated connectivity between the DLPFC and the IPC. This result agrees with findings from another DCM study in healthy controls that also showed a modulatory effect on fronto-parietal coupling in a working memory task [208]. In contrast, in patients with PD the model of best fit implies a different connectivity pattern, with both the DLPFC and IPC serving as driving regions with no task-modulated coupling. This finding fits our hypothesis that patients with PD employ a different and less-connected task-related network. A recent longitudinal analysis of MEG resting state data that compared graph theoretical network properties of PD patients over time similarly showed that already in the early stages the network topology is less efficiently organized, and becomes more fragmented with increasing disease duration [205]. Rowe and colleagues [209] also found that healthy participants increased effective connectivity between prefrontal and pre-supplementary motor areas during a motor sequence task, while the patients with PD showed no such task-specific modulation of this premotor network, suggesting a differently organized and less efficiently connected network. This altered network dynamic was also accompanied by hyperactivation of the pre-supplementary motor area, similar to the hyperactivation seen in conjunction with disrupted functional and effective connectivity in our own study. In that study dopaminergic medication restored the effective connections within the sample of Parkinson´s patients to those of healthy controls [210], further underscoring the role of dopamine in neural communication.

Contrary to our findings in the fronto-parietal network, we found no best-fit models of effective connectivity within the fronto-striatal network. Considering our hypothesized role of dopamine and the fronto-striatal system, this was unexpected. This may be due to a less specific role of the caudate nucleus in performing the task compared to baseline, as recent computational theories place the caudate nucleus in the role of action selection and updating working memory [211], disallowing a strong fit between our models and the data. The relatively small sample size

used for this network, however, may also be responsible for none of the models having a better fit than the others.

We hypothesize that PD patients in our sample, still in an early disease stage, compensate for a loss in connectivity and efficiency via hyperactivation, in a way that has been previously described to mask cognitive dysfunction in patients with PD [175, 212] as well as in multiple sclerosis patients [213]. Eventually, cognitive impairments become behaviourally evident when hyper-activation is either no longer able, or is insufficient to, compensate for the decreased connectivity.

Previous investigations have shown that dopaminergic medication alleviates at least some cognitive dysfunctions in patients with PD [214] and Parkinson patients display reduced activity in the ON state when compared with the OFF state during a working memory task [176]. We thus hypothesize that dopamine suppletion restores network connectivity and in this way cognitive performance.

Strengths and Limitations

Most previous study results are based on data from patients already on dopamine replacement therapy; as dopaminergic medication has a long-term negative effect on receptor density [215], the *de novo* nature of the present PD sample was an important methodological advantage allowing a more pure investigation of the disease process. In addition to the ROI analyses, we also presented the whole brain analyses (see supplemental material), in order to prevent overlooking significant findings in non-a priori hypothesised brain regions. As our sample of PD patients was relatively small, these results have to be replicated in future studies, and the causal role of dopamine in network integrity and task performance must be confirmed with an ON vs. OFF medication study, or a longitudinal study on the effects of dopamine replacement therapy on task-related connectivity. As a number of patients were excluded prior to scanning due to an inability to perform the task at all, our sample may also represent a more cognitively intact subgroup, which may also partly explain the only mild behavioural deficit that we observed. Finally, although our study focused on the role of dopamine, we cannot exclude the influence of other neurotransmitters or pathological atrophy as contributing factors to our findings

CONCLUSIONS

We hypothesize that the decrease in connectivity within the networks was compensated for by the hyper-activation of the individual task-related brain areas and

that this compensation underlies the relatively preserved working memory task-performance.

SUPPLEMENTARY FIGURES AND TABLES:

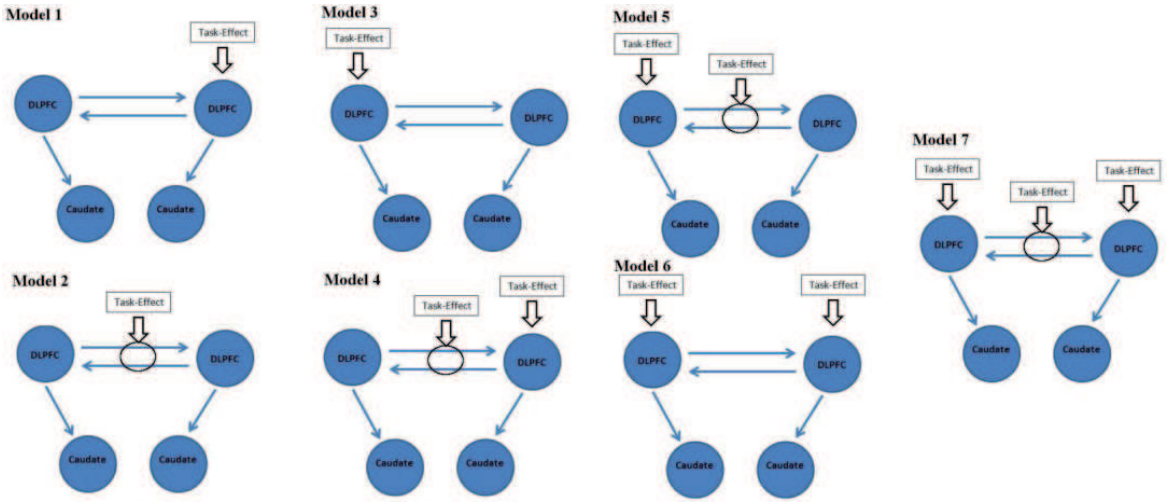

Figure S5.1. Fronto-striatal models used in DCM analysis. Blue arrows indicate intrinsic connections, black open arrows pointing towards a region indicates a driving effect on that region, and black open arrows pointing towards intrinsic connection-arrows indicates experimental modulation of connections falling within the black circle under the arrow.

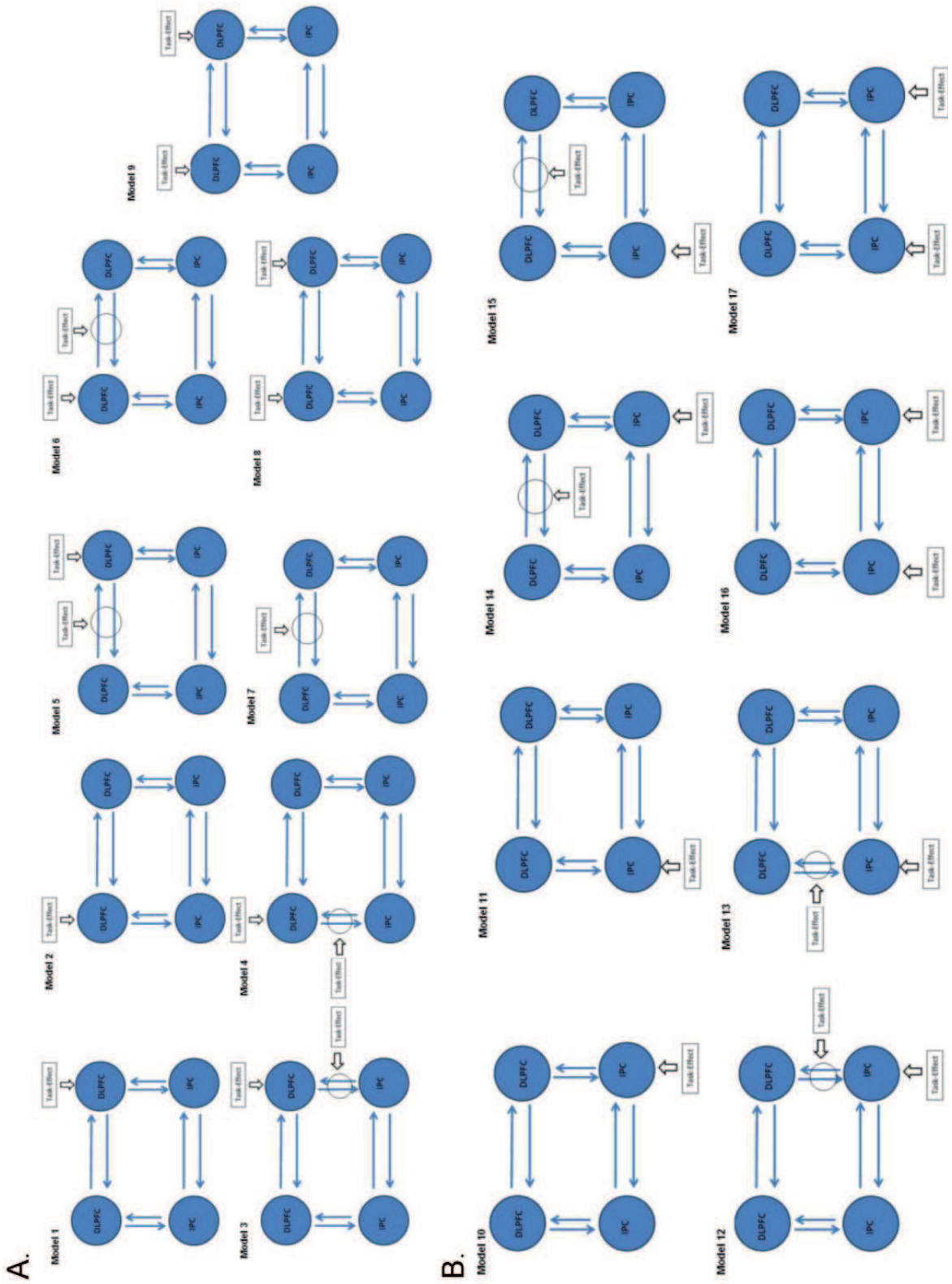
A.
B.
Model 1
Model 2
Model 3
Model 4
Model 5
Model 6
Model 7
Model 8
Model 9
Model 10
Model 11
Model 12
Model 13
Model 14
Model 15
Model 16
Model 17
DLPFC
IPC
Task-Effect

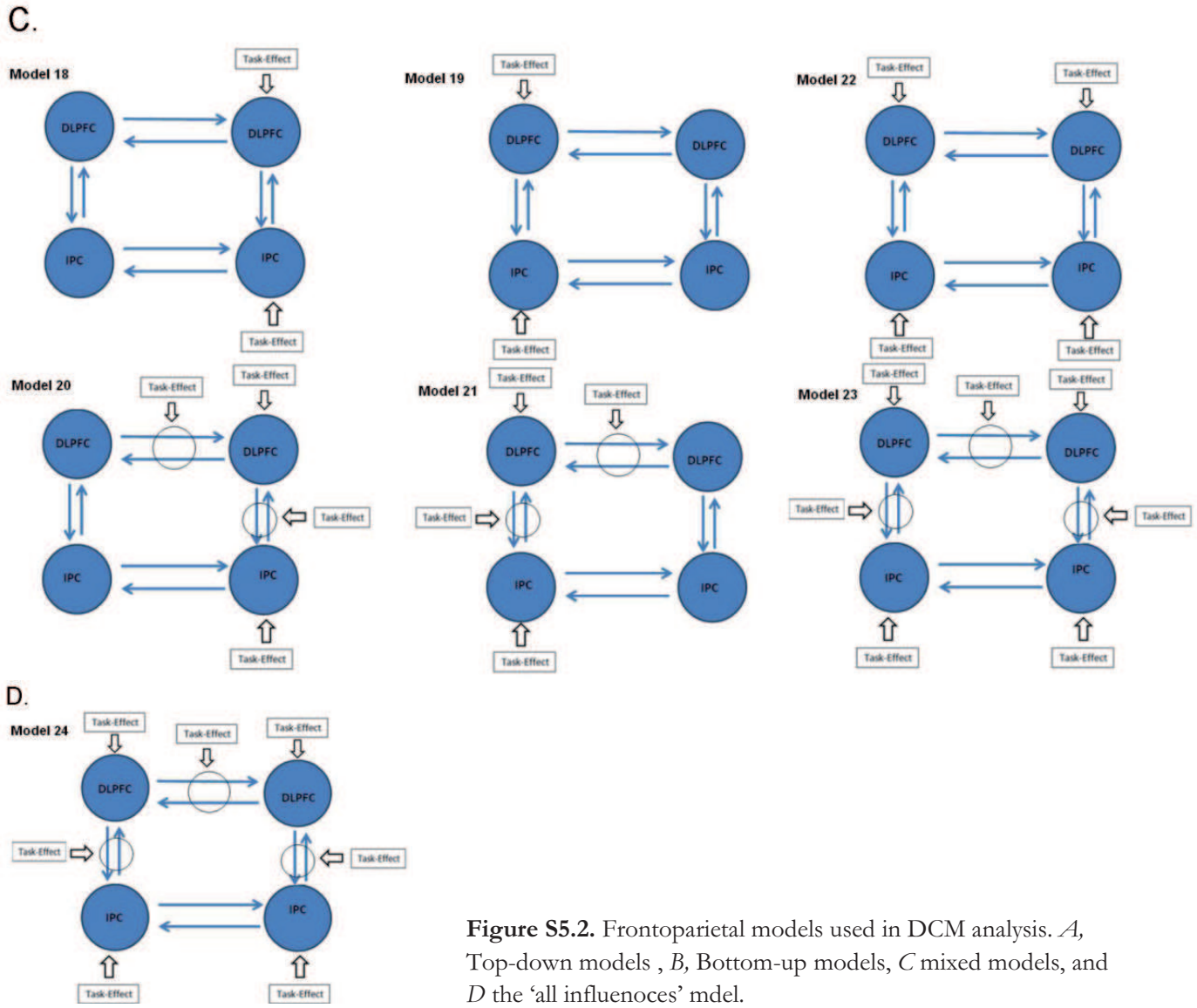

Figure S5.2. Frontoparietal models used in DCM analysis. *A,* Top-down models , *B,* Bottom-up models, *C* mixed models, and *D* the 'all influenoces' mdel.

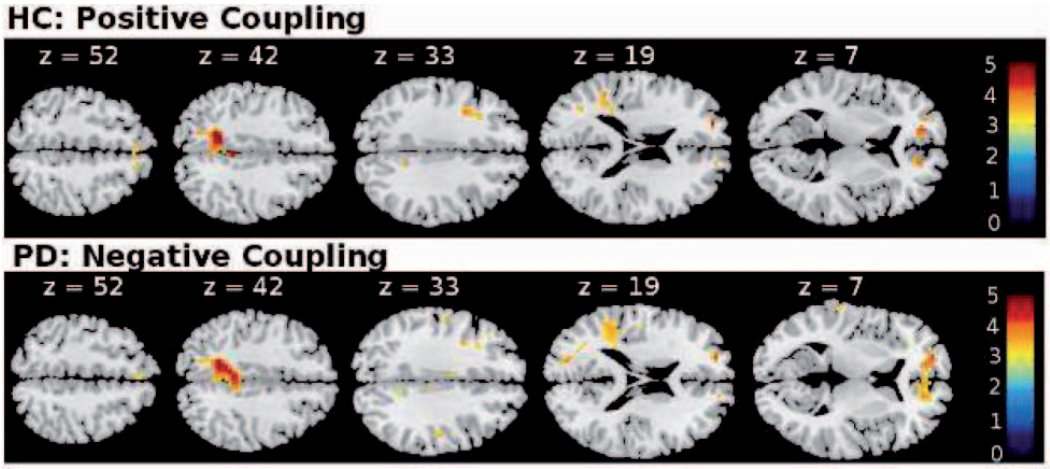

Figure S5.3 Functional connectivity maps showing opposite coupling in the controls and Parkinson's patients. On top, regions showing positive coupling with the left DLPFC are indicated on the horizontal slice of a standardized T1 MR image. On the bottom, regions showing positive coupling with the left DLPFC are indicated on a standardized T1 MR image. Slice position is indicated in white text above each image. The colour gradient legend represents the Z-scores. Abbreviations: *DLPFC* dorsolateral prefrontal cortex; *HC* healthy controls; *MR* magnetic resonance; *PD* patients with Parkinson's disease

Supplementary Table 5.1: Whole brain main effect of task across all subjects (N = 51). Significant at a threshold of $p = .05$ (FWE-corrected) with an extent-threshold $k > 10$

BA	Area	T-value	Cluster size	Peak coordinates (MNI)		
				X	Y	Z
40	Inferior parietal cortex	12.34	4050	51	-55	40
40		10.81		-42	-52	43
7	Precuneus	11.93		36	-64	43
7		10.85		-9	-70	46
19	Cuneus	10.89		33	-76	28
19		9.96		-30	-76	22
37	Middle temporal gyrus	8.98		54	-61	1
8	Medial frontal gyrus	11.77	4224	-3	17	49
6	Middle frontal gyrus	9.61		-30	2	55
8	Superior frontal gyrus	10.58		3	14	55
6		10.05		18	11	61
10		10.31		33	53	16
44	Ventrolateral prefrontal cortex	10.12		51	11	19
47		6.08	76	-33	23	-2
9	Dorsolateral prefrontal cortex	9.58	4224	45	8	28
9		9.16		-42	26	31
	Cerebellum	7.06	14	-33	-67	-35
13	Insula	6.56	76	-30	20	10
22	Superior temporal gyrus	5.97	13	-51	14	-2
	Caudate nucleus	5.59	13	18	-4	16

Supplementary Table 5.2 Whole brain main effects of the task by group. Significant at a threshold of $p = .05$ (FWE-corrected) with an extent-threshold $k > 10$.

BA	Area	PD patients (n = 16)					Controls (n = 35)				
		T-value	Cluster Size	Peak coordinates (MNI)			T-value	Cluster size	Peak coordinates (MNI)		
				X	Y	Z			X	Y	Z
40	Inferior parietal cortex	9.33	2463	51	-55	40	9.05	1681	48	-52	43
40		7.91		-48	-52	49	8.16		-45	-49	43
7	Inferior parietal lobule						9.52		36	-64	46
7	Precuneus	7.84		15	-70	34	8.56		9	-64	52
19		7.48		30	-79	37					
7		8.14		-9	-73	46	7.51		-9	-70	46
40	Superior parietal lobule						7.51		-33	-73	46
39		8.42		36	-64	40					
7							6.19		-33	-64	55
21	Middle temporal gyrus	7.50		54	-61	1					
39		7.37		45	-73	10					
21		6.04		-51	-49	7					
46	Dorsolateral prefrontal cortex		62				8.22	275	-42	29	31
9		7.49		-51	17	28	7.32		-42	2	31
46		7.03	1919	42	47	10	9.31	1814	39	32	31
9		6.93		39	20	31	7.72		42	8	31
44	Ventrolateral prefrontal cortex	7.17		51	11	19	7.50		51	11	19
6	Superior frontal gyrus	7.57		3	11	55	7.87		15	5	64
8							7.75		3	14	55
6		7.34		0	2	64					
10		7.52		33	53	16	7.23		33	53	16
6	Middle frontal gyrus	7.25		24	14	58	7.66		33	5	58
6		7.22		-30	2	55					
8							8.29		-3	17	49
10		6.22	22	-33	50	16	5.26	275	-36	47	16

Supplementary Table 5.3. Whole brain significant group comparisons in the task-effect contrast. Significant at a threshold of $p = .001$ (uncorrected) with an extent-threshold $k > 5$

BA	Area	PD patients > Controls					Controls > PD patients				
		T-value	Cluster size	Peak coordinates (MNI)			T-value	Cluster size	Peak coordinates (MNI)		
				x	y	z			x	y	z
19	Middle occipital gyrus	4.09	140	36	-85	16					
22	Middle temporal gyrus	4.78	64	-51	-43	4					
21		3.66	13	60	-22	-5					
18	Cuneus	4.24	145	-12	-85	16					
9	Dorsolateral prefrontal cortex	4.17		-48	17	*25*					
29	Cingulate gyrus	4.12	14	15	-46	4					
31		3.60	16	15	-43	31					
22	Superior Temporal Gyrus	3.99	50	63	-31	16					
40	Inferior parietal cortex	3.94	14	-63	-40	22					
21	Middle temporal gyrus	3.66	13	60	-22	-5					
	Caudate nucleus	3.60	38	-12	-7	19					
7	Precuneus	3.39	8	18	-73	43					
7		3.54	14	-3	-67	46					

Supplementary Table 5.4. Whole-brain analysis of within-group gPPI effects for left DLPFC. Significant at a threshold of $p = .001$ (uncorrected) with an extent-threshold $k > 5$.

BA	Area	Controls ($n = 32$)					PD patients ($n = 15$)				
		T-value	Cluster size	Peak coordinates (MNI)			T-value	Cluster size	Peak coordinates (MNI)		
				X	Y	Z			X	Y	Z
				Positive Coupling							
8	Superior frontal gyrus	5.91	421	18	26	55					
6		4.99		-12	26	55					
6	Middle frontal gyrus	4.49		-33	8	58					
39	Middle temporal gyrus	4.76	130	-39	-58	22					
39	Angular gyrus	4.74	30	48	-73	34					
7	Precuneus	4.59	144	-3	-58	40					
9	Dorsolateral prefrontal gyrus	4.56	72	12	56	28					
		3.64	17	-33	17	34					

BA	Area	Controls (n = 32)					PD patients (n = 15)				
		T-value	Cluster size	Peak coordinates (MNI)			T-value	Cluster size	Peak coordinates (MNI)		
				X	Y	Z			X	Y	Z
				Negative Coupling							
46	Inferior frontal gyrus						5.53	245	-36	35	13
46							3.62				
							3.62	6	45	41	7
10	Superior frontal gyrus						5.53	245	-21	56	10
13	Insula						5.53		-27	20	16
31	Cingulate gyrus						5.36	141	-9	-40	43
23							3.70		6	-25	34
24							3.73	11	-6	29	19
32							3.52		-12	35	19
18	Cuneus						4.49	291	-18	-79	19
17							3.95	62	3	-85	10
18							3.75		15	-88	25
43	Postcentral gyrus						4.58	341	-51	-13	19
42	Superior temporal gyrus						4.47		-63	-25	10
22							3.67	24	57	-10	7
18	Lingual gyrus						4.41	43	0	-85	-14
18							3.34		15	-79	-14
40	Inferior parietal lobe						4.05	11	-57	-37	37
4	Precentral gyrus						4.04	17	48	-16	37
6							3.39		51	-4	10
19	Inferior occipital gyrus						3.81	32	42	-73	-8
37	Middle temporal gyrus						3.47		45	-61	-5
7	Precuneus						3.80	18	18	-79	40
	Putamen						3.73	6	-21	-4	19
44	Ventrolateral prefrontal cortex						3.72	7	57	8	16
	Cerebellum						3.72	10	3	-49	-11
10	Medial frontal gyrus						3.66	25	6	50	7

Supplementary Table 5.5. Whole-brain analysis of within-group gPPI effects for right DLPFC. Significant at a threshold of $p = .001$ (uncorrected) with an extent-threshold $k > 5$.

BA	Area	Controls ($n = 14$)					PD patients ($n = 33$)				
		T-value	Cluster size	Peak coordinates (MNI)			T-value	Cluster size	Peak coordinates (MNI)		
				X	Y	Z			X	Y	Z
	Positive Coupling										
8	Superior frontal gyrus	4.53	48	-12	20	55					
6		4.37	49	21	23	55					
	Negative Coupling										
	Cerebellum						4.67	64	6	-52	-11
							3.89		18	-46	-11
13	Insula						4.53	27	30	23	-8
13							4.06	9	-45	-10	16
47	Ventrolateral prefrontal cortex						4.48	9	-30	23	-11
	Thalamus						4.49	40	15	-25	-8
							4.27	47	-9	-31	-5
28	Parahippocampal gyrus						3.49		-15	-10	-11
	Amygdala						4.19	11	30	-7	-17
10	Middle frontal gyrus						3.89	16	-36	38	13
18	Cuneus						3.89	19	-12	-79	22
40	Inferior parietal lobe						3.78	14	-54	-37	40